DEVELOPMENT OF A HIGH BRIGHTNESS ION SOURCE

A.J.T. Holmes and M. Inman
Culham Laboratory, Abingdon, Oxon. OX14 3DB, U.K.
(Euratom UKAEA Fusion Association)

SUMMARY

The brightness and emittance of an ion beam can depend on the ion temperature, aberrations and scattering, as well as other factors. However, it is the ion temperature which determines the irreducible minimum value of the emittance and hence brightness, as the other components can be eliminated by careful design.

In this paper an ion source design is presented which has attained this minimum value for the emittance; the dependence of the ion temperature on the plasma source parameters is discussed.

THE ION SOURCE

Figure 1 presents an illustration of the ion source, which comprises the plasma generator and ion acceleration structure. Both of these components have been developed at the Culham Laboratory as part of an ongoing program for the injection of intense neutral atom beams into magnetically confined plasmas, for controlled thermonuclear research.

The plasma source is of the magnetic multipole type[1,2] sometimes called a "bucket" source, which has the advantages of a very high electrical efficiency, a low gas operating pressure and the production of a large volume of quiescent plasma. All these advantages arise from the magnetic multipole method of plasma confinement, which creates a magnetic well on all sides except the beam extraction surface, where the magnetic field is virtually zero.

The electrical efficiency is such that each kilowatt of arc power produces typically 4 amps of ions (in hydrogen) over the entire extraction area of about 80 cm^2. The uniform plasma area is about 40 cm^2 and is large enough, as can be seen in Fig. 1, for a multi-aperture extraction system, which is capable of giving a beam current of about 1 ampere. In these experiments, however, only a single aperture is used.

The gas pressure for reliable source operation can be as low as 2 m Torr; the electric efficiency does decrease, however, at this pressure, which minimizes the effects of scattering collisions in the extraction system. Hence, these collisions do not influence the beam emittance.

The ion extraction system is of the tetrode type; an illustration is shown in Fig. 2. The tetrode structure reduces the effects of the anode hole effect, by decoupling the extraction from the post acceleration gap, which raises the beam to its final energy. It also adds an additional electrostatic lens to the system, which enables the beam to be extracted with negligible compression. The divergence of the extracted ion beam depends on the degree of space charge neutralization, which in turn, depends on the diameter of the extracted beam.[3] Thus tetrode extraction systems have a big advantage as there is little beam compression and large diameter apertures can be used, as the anode hole effect is weaker.

The extraction geometry developed at Culham, shown in Fig. 2, has 12-mm diameter apertures, which are suitable for beam energies up to 70-80 kV. The maximum beam current through a single aperture extracted so far is 230 mA of mixed species H-ions at 70 kV, or 150 mA He^+ at the same energy. The extraction geometry is designed with water cooling, so that it can operate continuously. The beam divergence angle is 0.5^o, which arises from the finite ion temperature and residual space charge. Figure 2 also shows the calculated ion trajectories, and as can be seen, there is little aberration with this extraction geometry because of the flat plasma boundary and the large aperture in the second electrode.

Hence, the only contribution to the beam emittance arises from the finite ion temperature in the plasma source. This is discussed later, where it is shown that the observed temperatures can be explained by purely classical processes. The field-free plasma and its quiescent uniform behavior, make it unlikely that any non-linear processes contribute to the emittance.

BEAM EMITTANCE AND ION TEMPERATURE

The normalized emittance and brightness for a cylindrical beam are defined as:

$$\varepsilon_n = \beta\gamma\, A(r,r')/\pi$$

$$B_n = 2I_b/\pi^2\varepsilon_n^2 \quad ,$$

where I_b is the beam current. The ion temperature gives rise to a Maxwellian velocity distribution; hence the emittance of a non-relativistic beam of this type at the 1/e intensity contour at the extraction aperture is:

$$\varepsilon_n = \frac{4a}{\pi} \cdot \left(\frac{2e\,T_i}{m_i\, c^2} \right)^{1/2} \quad , \qquad (1)$$

and the diagram is rectangular in shape. The brightness is, hence:

$$B^2 = I_b\, m_i c^2/16a^2\, eT_i$$
$$= \pi J_i m_i c^2/16\, eT_i \quad , \qquad (2)$$

where J_i is the current density at the plane of extraction. The value of J_i depends on the extraction voltage and inter-electrode gaps and is only limited by the voltage breakdown strength of the extraction geometry.[4]

The ion temperature has been derived from the measured emittance, using Eq. 1 over a range of extracted current densities for both hydrogen and helium, as shown in Fig. 3. In the hydrogen discharge, a considerable rise in the value of T_i with increasing values of j_i is observed. Such an increase is not seen in a helium discharge, which suggests that there is a correlation between the increasing ion temperature and the increasing proton yield (also shown in Fig. 3). This may arise since the protons are more energetic than the other ions, because of their dissociation energy.

An emittance diagram of the hydrogen beam is shown in Fig. 4 for a beam energy of 40 keV. The normalized emittance for H_2^+, the average ion mass, is 0.12 πmm-mrad, which leads to a temperature of 0.68 eV and a brightness of 5.10^{11} mA/cm^2/steradian. Also shown in Fig. 5, is the output from the diagnostic device, which shows that both the beam spatial and angular profiles are gaussian in shape. The helium beam emittance for the same extraction geometry is much lower, only 0.055 πmm-mrad, which corresponds to a temperature of 0.32 eV and a brightness of 1.4×10^{12} mA/cm^2/steradian.

DISCUSSION

The ion temperature is determined by the gas temperature in the source, the heating caused by classical ion-electron coulomb collisions, thermalization of the plasma potential energy, and the cooling effects caused by charge-exchanging collisions. In addition, in hydrogen discharges the dissociation energy released in the reaction:

$$H_2^+ + e \rightarrow H^+ + H + e$$

must also be considered. Non-classical ion heating processes, such as electron beam-plasma interactions, are not considered, as they do not generate the observed Maxwellian (or gaussian) velocity distributions.

From the work by Spitzer,[5] the rate-of-change of ion energy with time is:

$$\frac{dU_i}{dt} = C\, n_e/T_e^{1/2}\, m_i \quad \left[Js^{-1}\right] , \qquad (3)$$

in the limit where T_e is much greater than U_i. The constant C, for electron collisions is 2.17×10^{-57} in mks units. Ion-ion collisions transfer energy far more rapidly, in the ratio of m_i/m_e. Hence, all the ions in the plasma have virtually the same temperature, although small differences in beam profile have been observed between the various hydrogen ion species.[6]

Before Eq. 3 is integrated, the cooling effects of charge exchange must be considered, which convert energetic ions into cool ions, while the fast neutrals, so formed, escape. However, if the discharge is large enough, these fast neutrals undergo a second charge-exchanging collision and re-form the original hot ion. As the cross-section is the same in both cases, the energetic particle spends half the distance it travels in the form of an ion and the other half in the form of a fast neutral atom or molecule.

However, the distance an ion travels in the plasma source, S_i, is a function of the source geometry alone. In the case of a bucket source:

$$S_i = \frac{A_T\, d}{A_i} ,$$

where A_T is total surface area, A_i is the ion collection area and d is the plasma diameter. Hence, the effect of charge-exchange collisions is to reduce the distance during which ions can be heated, to $S_i/2$. This conclusion is in agreement with experiment, as no variation in T_i was observed by varying the source pressure.

It is now possible to evaluate U_i by integrating Eq. 3. The equation can be transformed to:

$$\frac{dU_i}{dt} = \frac{dU_i}{ds}\left(\frac{2U_i}{m_i}\right)^{1/2} = \frac{C\, n_e}{T_e^{1/2} m_i} .$$

$$\text{Hence, } \frac{2}{3}\,(U_i)^{3/2}\left(\frac{2}{m_i}\right)^{1/2} = \frac{C n_e S_i}{2T_e^{1/2} m_i} + \text{constant} . \qquad (4)$$

The constant is defined by the initial temperature of the ions, which depends on the gas temperature, the proton fraction, and lastly, the plasma potential. The first and last of these are constant and do not depend on n_e; however, the proton fraction does depend on the ion current density, which is proportional to n_e. Hence, the initial energy, U_{io}, is:

$$U_{io} = 1/2\, m_i v_o^2 + \beta k T_e + fT = E_o + fT , \qquad (5)$$

where v_o is the gas temperature, β is a numerical factor, which is small compared to unity, f is the fractional proton yield and T is the dissociation energy. The term E_o, is virtually invariant to all changes in the discharge parameters.

Combining Eq. 4 and Eq. 5 gives:

$$U_i^{3/2} - (E_o + fT)^{3/2} = \frac{3C\, n_e\, S_i}{4(2m_i T_e)^{1/2}} = \frac{3C\, J_i\, S_i}{4(2k)^{1/2} e T_e}\,[J]^{3/2} , \qquad (6)$$

where U_i is the final ion temperature at extraction, assuming ions leave the plasma at the ion sound speed.

Equation 6 shows that the RHS is independent of the gas except for T_e, which is unlikely to vary greatly. For helium, there is no dissociation; hence, f is zero and Eq. 6 can be linearized when the RHS is small, to give:

$$U_i = E_o + \frac{2J_i}{3}\cdot\left(\frac{3\, C\, S_i}{4.(2k)^{1/2} e T_e\, E_o^{1/2}}\right) .$$

This expression can be tested against the helium data shown in Fig.6. The slope gives a value of 5.4×10^{-23} Jm^2/A, which is in reasonable agreement with the equation above, which yields a value of 5.7×10^{-23} Jm^2/A.

The hydrogen discharge is more difficult to analyze, but the value of U_i for H and He can be compared at the same current density. Thus, as the RHS is mass independent, and the electron temperature is constant, then:

$$U_{iH}^{3/2} - U_{iHe}^{3/2} = (E_{oH} + fT)^{3/2} - E_{oHe}^{3/2} \quad ,$$

or

$$(U_{iH}^{3/2} - U_{iHe}^{3/2} + E_{oHe}^{3/2})^{2/3} = E_{oH} + fT.$$

This is plotted in Fig.7 and a straight line is obtained. The slope of the line indicates that T is approximately 0.6 eV and E_{OH} is 0.22 eV, the same value as E_{oHe}.

The energy level diagram of H_2^+ shows that the full Frank-Condon energy between the $1S\sigma_g$ level (H_2^+) and the unstable $2P\sigma_u$ level ($H^+ + H^o$) depends very strongly on the vibrational level occupied by the H_2^+ ion. The small value of T suggests that H_2^+ ion is excited to a high vibration level in the $1S\sigma_g$ level before it is dissociated to the $2P\sigma_u$ level by electron impact. The Frank-Condon energy appears in the kinetic energy of the two daughter particles and hence this energy is 1.2 eV.

The value of E_o corresponds to 2500^{o}K for both H and He discharges. An estimate for β, based on the ionization rate and the plasma size, is in the region of 0.04, which suggests that βkT_e forms the major contribution to the value of E_o. The gas temperature in this small source could be close to room temperature because of the high collision rate with the source walls.

CONCLUSION

Extraction of ions from a quiescent plasma source, using a specially designed tetrode extraction system with a single aperture, allows ion beams to be formed whose emittance and brightness are only limited by the ion temperature. This temperature is mainly determined by the H_2^+ dissociation energy in hydrogen discharges and by the ion-electron collision rate in helium discharges, where ion dissociation does not occur.

Such ion temperature dominated beams are presently being used for neutral injection experiments in controlled thermonuclear fusion, but could be used in other applications.

ACKNOWLEDGEMENTS

The author would like to thank Dr T.S. Green for his encouragement in this work.

REFERENCES

1 Limpaecher, R, and Mackenzie, K R, Rev. Sci. Inst. 44, 726 (1973).

2 Hemsworth, R S., Culham Report CPNI-CUL(77)8.

3 Holmes, A J T. Phys. Rev. A, 19, 389 (1979).

4 Green, T S. Rep. Prog. Phys. 37, 1257 (1974).

5 Spitzer, L. Physics of Fully Ionized Gases, Wiley, 1967, New York.

6 Holmes, A J T, Thompson, E. & Watters, F., to be published.

7 Massey, H S W.,"Electronic & Ionic Collision Phenomena", 2, 914, O.U.P., Oxford (1969).

FIG 1

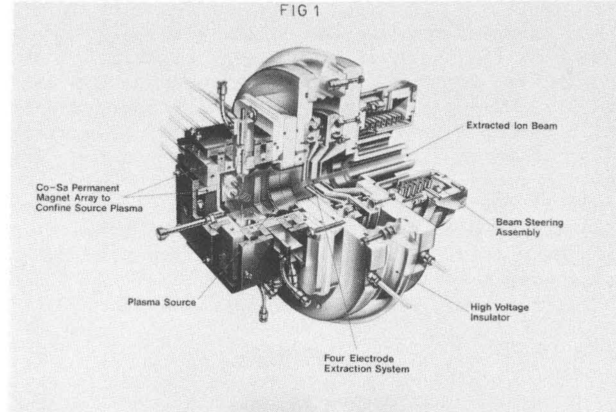

Fig.1 Cut-away view of ion source

FIG 2

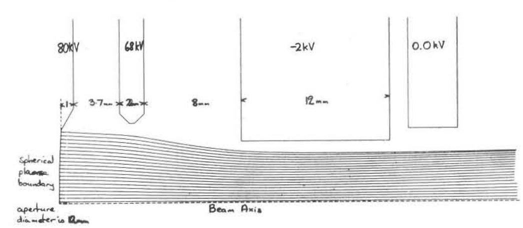

Fig.2 Numerical view of ion trajectories

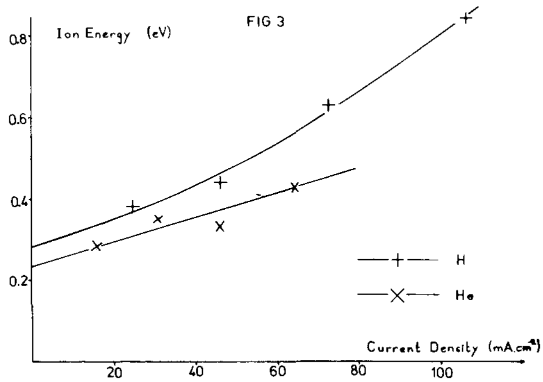

Fig.3 Measured ion temperature of ion derived from beam emittance in hydrogen and helium discharges as a function of ion current density

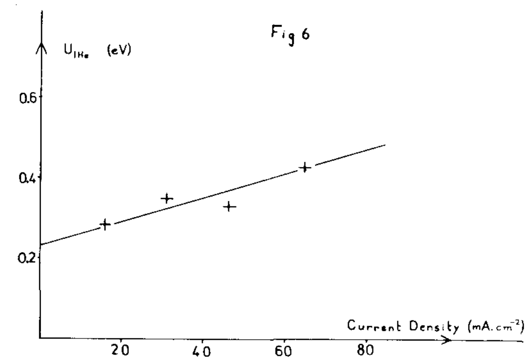

Fig.6 Scaling of the helium temperature with ion current density

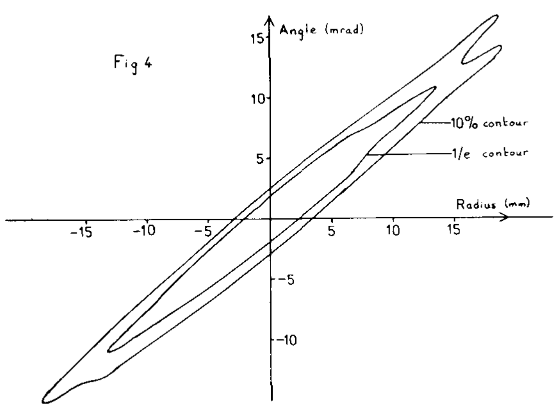

Fig.4 Typical emittance diagram

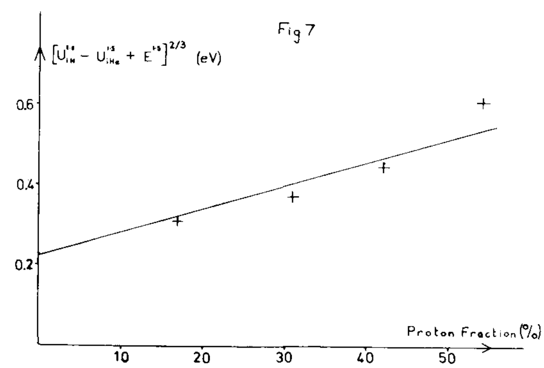

Fig.7 Scaling of hydrogen temperature with fractional proton density

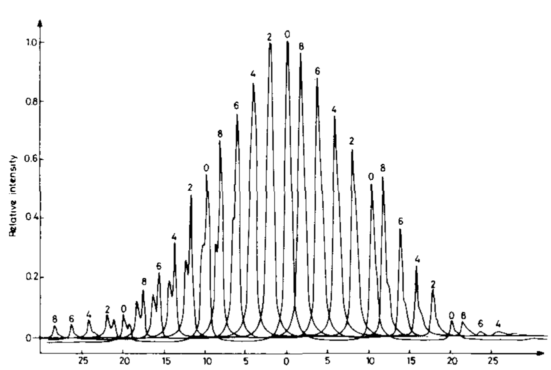

Fig.5

Fig.5 Raw data from emittance device showing the gaussian beam profile and the individual peaks